IEEE Access
Multidisciplinary | Rapid Review | Open Access Journal

IEEE POWER & ENERGY SOCIETY SECTION

Received 21 August 2022, accepted 11 September 2022, date of publication 16 September 2022,
date of current version 26 September 2022.

*Digital Object Identifier 10.1109/ACCESS.2022.3207297*

RESEARCH ARTICLE

# An Improved Model Predictive Fast Frequency Control for Power System Stability Against Unknown Time-Delay Switch Attack

**RAMADHANI KURNIAWAN SUBROTO[1], (Member, IEEE), AND KUO LUNG LIAN[2], (Senior Member, IEEE)**

[1]Department of Wind and Energy Systems, Technical University of Denmark, 2800 Kongens Lyngby, Denmark
[2]Department of Electrical Engineering, National Taiwan University of Science and Technology, Taipei 106, Taiwan

Corresponding author: Kuo Lung Lian (ryankuolian@gmail.com)

This work was supported in part by the National Science and Technology Council, under Grant 110-2221-E-011 -158 -, and in part by the Taiwan Building Technology Center from the Featured Areas Research Center Program within the framework of the Higher Education Sprout Project by the Ministry of Education in Taiwan.

**ABSTRACT** A modern power grid is a cyber-physical system, which are vulnerable to cyber attacks. A recently found attack, the time-delay switch attack (TDSA), is made by inserting time delays into communication channels. A TDSA can be highly destructive to a power system as it can lead to instability. This paper presents a novel model predictive control (MPC) for fast frequency controller in a power system which can effectively mitigate the unknown TDSA. The MPC recently has received great attentions to be applied as FFC in a power system. Most of the MPC design are based on discrete-time model, whose future plant behaviour is calculated through iteration, rather than convolution. Nevertheless, one crucial step in the derivation of discrete-time MPC (DTMPC) is to capture the control trajectory over a finite prediction horizon. This imposes a challenge in designing a DTMPC to counteract the time-delay with unknown time length. Thus, a continuous-time MPC (CTMPC) is proposed to deal with TDSA. To overcome the unknown time delay, we synthesize an accurate time-delay estimator and sequential state predictor (SSP), are designed to accurately estimate and effectively counteract the unknown and random TDSA. All presented case studies are based on a real Taipower system and justification of the effectiveness of the proposed method was verified.

**INDEX TERMS** Energy storage, frequency regulation, model predictive control, sequential state predictor, time-delay switch attack, time-delay estimation.

## NOMENCLATURE

| | |
|---|---|
| $\tau(t)$ | unknown round trip time delay. |
| $\hat{x}(t)$ | estimated state variable variables. |
| $\hat{\tau}$ | estimated time-delay. |
| $N$ | order of sequential state predictor. |
| $H$ | inertia constant. |
| $D$ | damping coefficient. |
| $T_g$ | governor-turbine constant. |
| $R_g$ | equivalent droop constant. |
| $\tilde{P}_m$ | change of mechanical power. |
| $P_{ESS}$ | power of energy storage system. |
| $\dot{P}_{ESS}$ | rate of power of energy storage system. |
| $\tilde{P}_e$ | change of electrical power. |
| $\tilde{f}$ | frequency deviation. |
| $K_{ob}$ | observer gain. |
| $K_{SPN}$ | state predictor gain. |
| $K_{mpc}$ | control gain. |
| $z(t)$ | approximation of the predicted state. |
| $m(t)$ | external signal. |
| $C^0$ | the set of all continuous functions. |
| $C^1$ | the set of all functions whose derivative are in $C^0$. |
| $\sigma(t)$ | sliding surface. |
| $l_i(t)$ | orthonormal basis functions $i$. |
| $r$ | the number of Laguerre networks. |
| $L(t)$ | Laguerre function. |
| $\lambda$ | time scaling factor for the Laguerre functions. |
| $J$ | expression of the cost function. |
| $Q$ | weighting matrix of predicted state. |
| $T_p$ | horizon of predicted time. |

The associate editor coordinating the review of this manuscript and approving it for publication was Suman Maiti.

| | |
|---|---|
| $\varphi$ | an arbitrary future time. |
| $R$ | weighting matrix of input. |
| $k$ | step size. |
| $y_{max}$ | minimum frequency deviation. |
| $y_{min}$ | maximum frequency deviation. |
| $\alpha_1, \alpha_2$ | parameters of super-twisting time-delay estimator. |
| $P_{C,max}$ | Maximum energy storage system (ESS) charging power. |
| $P_{D,max}$ | Maximum ESS discharging power. |
| $P_{RR,dn}$ | Maximum downward ramp rate. |
| $P_{RR,up}$ | Maximum upward ramp rate. |

## I. INTRODUCTION

A modern power grid, taking advantages of advanced control strategies, cost-competitive technologies and information and communication technology (ICT), is a cyber-physical systems (CPSs), which are vulnerable to cyber attacks. Some of the well-known cyber-attacks are denial of service, which disables access to the system information or a service, false data injection, which intentionally manipulates the exchange of data, replay attack, which maliciously repeats valid data transmission [1]. A recently found attack, the time-delay switch attack (TDSA) [2], is made by inserting time delays into communication channels of CPSs.

A TDSA can be highly destructive to a power system as it can lead to instability [3]. The critical time-delay reflects the maximum time-delay causing the system to be marginally stable. If the specified critical time-delay is smaller than the allowable communication time-delay, then the power system is unstable. Moreover, power systems may also introduce uncertainties depending on their operations, which particularly change the critical time-delay. This change may potentially reduce the allowable time-delay limit, which reflects on the communication time-delay. In this way, the stability of the power systems can be degraded. Several strategies have been proposed to deal with time-delay issues, in which the majorities concern on load frequency control (LFC) problem. In [4], an LFC based PI controller is implemented to regulate the system frequency after unpredictable contingency. This work investigated the maximum allowable critical time-delay, which can be withstood by the PI controller. Similar works have been done by [5], [6], [7], [8], which employ PI controllers for LFC applications. These works are more concentrated in the investigation of stability boundaries caused by the time-delay. In [9], Fu *et al.* proposed a filter-based method to compensate the communication time-delay issue. Even though this method can enlarge the critical time-delay to some extent, the robustness against the random TDSA has not been ensured yet. A method to counteract random time-delay attack based on perturbation observer has been devised by [10]. In their work, the random time-delay is assumed as an unknown disturbance, whose effect is necessary to be minimized to some degree. Although this method does not require to exactly estimate the time-delay values to tune the control parameters, this method is not able to compensate relatively long time-delay. It is to be noted that the methods proposed by [4], [5], [6], [7], [8] merely evaluate the maximum critical time-delay by selecting the appropriate control parameters. Nevertheless, in practice, the TDSA can be time-varying and random, which makes the work of [4], [5], [6], [7], [8] not applicable to counteract the time-varying and random TDSA. Two approaches for compensating the TDSA are by redesigning the controller to satisfy the robustness and by estimating the unknown TDSA without the need of redesigning the controller. The first approach is prone to be unstable if the TDSA is larger than the specified critical-time delay. The second approach, on the other hand, is intended to estimate the unknown TDSA and compensate the time-delay. There are studies for estimating time delays, and they can be generally classified into five approaches, which are optimization-based, convolution-based algebraic, adaptive backstepping-based, artificial intelligence-based, and sliding mode-based. In the optimization-based, the estimated time-delay is an optimal solution obtained based on a cost function minimization. Some studies related to optimization-based approach can be found in [11], [12], [13], [14], [15], and [16]. For example, in [15], input and output time-delays are lumped into a round trip time (RTT) delay and a time-delay estimator (TDE) is proposed to estimate the unknown RTT delay in a linear system. In [2], the authors used gradient descent method to estimate the delay by minimizing the modelling error signals. Furthermore, in [16], the TDE is proposed to estimate the unknown time-delay in dc motor applications. Nevertheless, these methods are unable to estimate fast time-varying and random time-delay. In the convolution-based algebraic approach, the convolution method is applied to identify the unknown parameters and constant delay of a linear system. This approach provides high convergence, but it is not applicable to time-varying or random time-delay estimation. Some studies related to this approach are covered in [17], [18], and [19]. The third approach, which is a class of nonlinear systems, applies partial differential equation (PDE) transformation to estimate the unknown time-delay. For instance, in [20], [21], and [22], an adaptive backstepping-based TDE method is attempted to regulate an unstable system. Nevertheless, this method is only able to estimate the constant time-delay and the convergence highly depends on the initial conditions. In the artificial intelligence-based approach, a neural network (NN) is used to estimate the unknown time-delay [23], [24]. However, this method is only able to estimate constant time-delay and requires a large set of data for training. Moreover, as pointed out in [1], the NN-based methods are prone to maliciously altering the training data and cause disastrous operation and system instability. The sliding mode-based TDE was first developed by [25] to estimate the unknown, fast time-varying and random time-delay. This estimator is similar to the concept of sliding mode control, in which the sliding surface is employed and defined as a function of external signal difference. The external signal is basically a function of time, which specifically can be a clock. In [25],

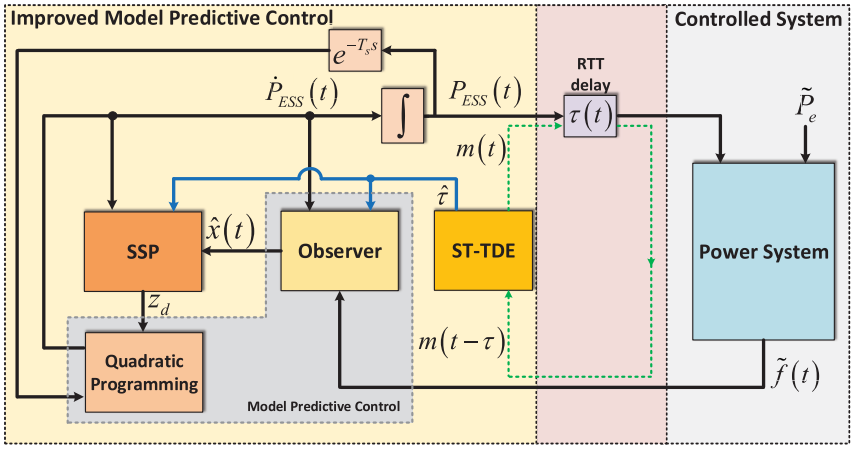


**FIGURE 1.** Block diagram of the proposed method.

variable structure-like estimator is devised to estimate the unknown and random time-delay. This method is able to converge to the actual time-varying time-delay. Nevertheless, the estimated time-delay suffers from chattering due to switching functions, leading to inaccuracy. To enhance the effectiveness of this method, Deng *et al.* [26], [27] proposed a TDE based on super-twisting algorithm, which was first introduced by [28] for chattering suppression in conventional sliding mode control. This concept is subsequently extended for estimation problem by Deng *et al.*, aiming at reducing the chattering effect and improving the convergence time. This method provides superior performance in accurately estimating the unknown and random time-delay.

Generally, the above mentioned TDEs are verified using a simple state feedback controller. For instance, in [29], a delay-dependent robust method is proposed for analysis of a PID-type LFC scheme considering time delays. Recently, model predictive control (MPC) [30], [31], [32] has attracted great attention for power system controller because of its simplicity in developing the control strategy for a multi-input and multi-output system and its capability of dealing with various types of constraints imposed by the system [33]. Moreover, Chen *et al.* [34] shows that MPC based LFC controllers have low overshoot and fast response, compared to the conventional PI based. In addition, the MPC employed in [34] was discrete one and can only handle constant time delay. In this paper, we designed a MPC based fast frequency controllers (FFCrs), which can effectively counteract the frequency deviation using an energy storage system (ESS) for a low inertia system and is able to compensate for random and unknown time delay attack. To authors' knowledge, such an FFCr is currently not available. The main contributions of the paper are:

- It devises a MPC based FFCr which is capable of optimally allocating ESS power considering on its specifications and admissible frequency ranges.
- Different from most the MPC based controller, the proposed FFCr is based on continuous MPC; thus it can synthesizes super-twisting TDE into the controller to accurately estimate random TDSA injected by malicious adversary.
- It yields practicability as the proposed FFC is able to compensate TDSA without the need of redesigning the controller.
- It evaluates the robustness and effectiveness of the improved model predictive fast frequency controller under parameter changes and various TDSAs.

The paper is organized as follows. Section II describes the structure of the proposed FFC. Section III describes how various constraints are incorporated into the designed MPC to be applicable in a power system. Section IV specifies control parameters and the effect of system parameter changes on the critical time-delay. Case studies are presented in Section V. Conclusions are drawn in Section VI.

## II. PROPOSED CONTROL SYSTEM DESIGN

Fig. 1 depicts the block diagram of the proposed system, composed of the power system, acting as a plant, the unknown time-delay, and the proposed control method. The unknown time-varying time-delay constitutes lumps of input and output delays and is represented as a RTT delay. Furthermore, the proposed control method is composed of three subsystems, which are the super-twisting time-delay estimator (ST-TDE), sequential state predictor (SSP), and MPC, which consists of an observer and optimizer. The unknown RTT delay, $\tau\,(t)$, is estimated by ST-TDE to yield the estimated time-delay, $\hat{\tau}$. Then, the estimated time-delay is fed to the observer and SSP. The observer receives the measurement data, which are specifically the measured frequencies, to yield the estimated state variable $\hat{x}\,(t)$. The estimated state variable is subsequently processed by the SSP to predict the future state variable under a given estimated time-delay, which results in $z_N$. Note that $z_N$ is an approximation of $\hat{x}\,(t+\tau)$. The optimization algorithm, such as Quadratic Programming (QP) is employed to iteratively compute the optimal solution, which minimizes the given cost function under specified ESS power

limitations. The corresponding cost function is a function of the future state trajectory and ESS power. The resulting optimal solution is the time derivative of ESS power, $\dot{P}_{ESS}(t)$, which is then passed to an integrator to determine the required amount of power from the energy storage, $P_{ESS}(t)$.

### A. DESCRIPTION OF THE SYSTEM MODEL

In general, the aggregated PFR dynamics incorporated with the ESS power is formulated as [35]

$$\begin{aligned} \dot{x}_p(t) &= A_p x_p(t) + B_p\left(P_{ESS}(t) - \tilde{P}_e(t)\right) \\ y(t) &= C_p x_p(t) \end{aligned} \tag{1}$$

where

$$\begin{aligned} x_p &= \left[\tilde{P}_m \; \tilde{f}\right]^T \\ A_p &= \begin{bmatrix} -\frac{1}{T_g} & -\frac{1}{R_g T_g} \\ \frac{1}{2H} & -\frac{D}{2H} \end{bmatrix} \\ B_p &= \left[0 \; \frac{1}{2H}\right]^T \\ C_p &= \left[0 \; 1\right] \end{aligned} \tag{2}$$

Note that the PFR parameters, such as inertia constant $(H)$, damping coefficient $(D)$, governor-turbine constant $\left(T_g\right)$, and an equivalent droop constant $\left(R_g\right)$, are obtained via identification method, proposed by Subroto *et al.* [33]. $\tilde{P}_m$, $P_{ESS}$, $\tilde{P}_e$, and $\tilde{f}$ denote the mechanical power change, ESS power, electrical power change, and frequency deviation, respectively. We assume that the external disturbance is related to a zero mean, white noise sequence. Hence, based on [30], the predicted value of the difference of the disturbance at future sample i is assumed to be zero. The prediction of state variable and output variable is calculated as the expected values of the respective variables, hence, the noise effect to the predicted values being zero.

To minimize the steady-state error, an integrator can be embedded in (1), and an auxiliary variable is introduced as $v(t) = \dot{x}_p(t)$. Hence, the dynamics of $v(t)$ can be expressed as

$$\dot{v}(t) = A_p v(t) + B_p \dot{P}_{ESS}(t) \tag{3}$$

Note that $\tilde{P}_e$ is basically a step function and $\dot{\tilde{P}}_e = 0$. Also, the output state variable dynamics can be obtained as

$$\dot{y}(t) = C_p \dot{x}_p(t) = C_p v(t) \tag{4}$$

Augmenting (3) and (4) to the system yields

$$\begin{aligned} \dot{x}(t) &= Ax(t) + B\dot{P}_{ESS}(t) \\ y(t) &= Cx(t) \end{aligned} \tag{5}$$

where

$$\begin{aligned} x(t) &= \left[v(t) \; y(t)\right]^T \\ A &= \begin{bmatrix} A_p & 0 \\ C_p & 0 \end{bmatrix} \\ B &= \left[B_p \; 0\right]^T \\ C &= \left[0 \; I\right] \end{aligned}$$

Eq. (5) serves as an augmented system of (1) containing an integrator. To consider the existence of time-delay in (5), the dynamic representation of a time-delay system is expressed as

$$\dot{x}(t) = Ax(t) + B\dot{P}_{ESS}(t - \tau(t)) \tag{6}$$

where $\tau(t)$ is the unknown RTT time-delay. Note that since $\tau(t)$ is an unknown value, the estimation is carried out to obtain the estimated value of time-delay, $\hat{\tau}(t)$. Section II.B. discusses how the proposed ST-TDE can accurately estimate the unknown TDSA. Furthermore, the observer is applied to estimate the state-variables from the input and output variables. The observer dynamics is represented as

$$\begin{aligned} \dot{\hat{x}}(t) = A\hat{x}(t) + B\dot{P}_{ESS}\left(t - \hat{\tau}(t)\right) + K_{ob} \\ \times \left(y(t) - C\hat{x}(t)\right) \end{aligned} \tag{7}$$

where $K_{ob}$ is the observer gain, whose value is determined via pole-placement technique.

### B. SEQUENTIAL STATE PREDICTOR

SSP is devoted as a countermeasure to deal with a relatively long time-delay system. This method is also well-known as a chain predictor. The term "long" is used to describe the time-delay, which is larger than the critical time-delay. To circumvent this problem, this approach extends a sequential prediction containing copies of the system dynamics which run at different time scale.

The concept of this approach resembles a basic predictor, which essentially provides the estimation of the predicted state, $x(t+\tau)$. Without loss of generality, $z(t)$ is defined as the approximation of the predicted state, $x(t+\tau)$. In [36], the SSP is expressed as a set of successive estimation of $x\left(t + i\frac{\tau}{N}\right)$, where $i = 1, 2, \ldots, N$ defines the number of set. Accordingly, the SSP dynamics are represented as

$$\begin{aligned} \dot{z}_1(t) &= Az_1(t) + B\dot{P}_{ESS}(t - k_1\tau) + K_{SP1} \\ &\quad \times \left[z_1\left(t - \frac{\tau}{N}\right) - x(t)\right] \\ \dot{z}_2(t) &= Az_2(t) + B\dot{P}_{ESS}(t - k_2\tau) + K_{SP2} \\ &\quad \times \left[z_2\left(t - \frac{\tau}{N}\right) - z_1(t)\right] \\ &\vdots \\ \dot{z}_N(t) &= Az_N(t) + B\dot{P}_{ESS}(t) + K_{SPN} \\ &\quad \times \left[z_N\left(t - \frac{\tau}{N}\right) - z_{N-1}(t)\right] \end{aligned} \tag{8}$$

where $k_i = \frac{N-i}{N}$ for $i = 1, 2, \ldots, N$ and $K_{SP1}, K_{SP2}, \ldots, K_{SPN}$ denote the predictor gain for $i = 1, 2, \ldots, N$, respectively. For simplicity, one may select $K_{SP1} = K_{SP2} = \ldots = K_{SPN}$. As $\tau(t)$ is unknown, the estimated time-delay, $\hat{\tau}$, yielded from ST-TDE is used. Moreover, as $x(t)$ is not readily available, $\hat{x}(t)$ obtained from the observer, i.e. (7) is employed. Consequently, SSP in (8) can be modified into (9).

$$\dot{z}_1(t) = Az_1(t) + B\dot{P}_{ESS}\left(t - k_1\hat{\tau}\right) + K_{SP1}$$

$$\times [z_1 \left(t - \frac{\hat{\tau}}{N}\right) - \hat{x}\,(t)]$$
$$\dot{z}_2\,(t) = Az_2\,(t) + B\dot{P}_{ESS}\left(t - k_2\hat{\tau}\right) + K_{SP2} \times [z_2 \left(t - \frac{\hat{\tau}}{N}\right) - z_1\,(t)]$$
$$\vdots$$
$$\dot{z}_N\,(t) = Az_N\,(t) + B\dot{P}_{ESS}\,(t) + K_{SPN} \times [z_N \left(t - \frac{\hat{\tau}}{N}\right) - z_{N-1}\,(t)] \quad (9)$$

$z_N$ can be obtained by integrating (9) so as to obtain the time derivative of th ESS power, $\dot{P}_{ESS}$. Accordingly, the control law of IMP-FFC without constraints can be directly obtained as

$$\dot{P}_{ESS}\,(t) = K_{mpc}z_N\,(t) \quad (10)$$

where $K_{mpc}$ is the control gain, whose value can be obtained by minimizing a cost function with respect to the control input. In this study, we will show that $K_{mpc}$ defined for a time-delay system is similar to that defined in a delay-free system. Detailed discussion of the control gain calculation is presented in Section III.

### C. SUPER-TWISTING TIME-DELAY ESTIMATOR

Several attempts to improve the accuracy of TDE techniques have been conducted by [15], [16], [25], [26]. Among the TDE techniques, super-twisting time-delay estimator (ST-TDE) offers numerous advantages because it is able to estimate random time-delay. ST-TDE essentially employs the concept of sliding mode control, in which the sliding surface is constructed as an attempt to drive the error states to stay in the equilibrium. The sliding surface is defined as

$$\sigma\,(t) = m\left(t - \hat{\tau}\,(t)\right) - m\,(t - \tau\,(t)) \quad (11)$$

where $m\,(t)$ is an external signal, which satisfies $m\,(t) \in C^1$. Note that $C^1$ is the set of all functions whose derivatives are in $C^0$, and $C^0$ is the set of all continuous functions. Thus, for simplicity, we define $m\,(t) = t$.

ST-TDE dynamics can be represented as

$$\dot{\hat{\tau}}\,(t) = 1 - \frac{1}{\dot{m}\left(t - \hat{\tau}\,(t)\right)}h\,(t) \quad (12)$$

where

$$h\,(t) = -\alpha_1|\sigma\,(t)|^{\frac{1}{2}}sgn\,(\sigma\,(t)) - \alpha_2\int sgn\,(\sigma\,(t))dt \quad (13)$$

where $\alpha_{1,2} > 0$ are positive constants. Compared to [25], this approach shares some advantages i.e. fast convergence speed, less chattering, and minimum steady-state error for time-varying TDE.

## III. MODEL PREDICTIVE FAST FREQUENCY CONTROL

In this section, we will describe how the developed MPC can be applicable to a practical power system. Most of the MPC design are based on discrete-time model, whose future plant behaviour is calculated through iteration, rather than convolution. Nevertheless, one crucial step in the derivation of discrete-time MPC (DTMPC) is to capture the control trajectory over a finite prediction horizon. This imposes a challenge in designing a DTMPC to counteract the time-delay with unknown time length. Thus, a continuous-time MPC (CTMPC) is proposed to deal with TDSA. In section III-A, we will show the trajectory of the continuous control variable can be described by means of Laguerre functions so that the CTMPC can be solved in a similar fashion to the DTMPC without considering the system constraints. In section III-B, we will then incorporate the system constraints to the developed CTMPC to be applicable in a practical power system.

### A. MODEL PREDICTIVE FAST FREQUENCY CONTROL WITHOUT CONSTRAINTS

Recall that the input of the augmented system (5) as the derivative of the control, $\dot{P}_{ESS}\,(t)$. This condition implies that the bounded input and bounded output stability is achieved if $\lim_{t\to\infty}\dot{P}_{ESS}\,(t) = 0$. This condition leads to the convergence of the control signal to its steady-state value, which can be represented as

$$\lim_{t\to\infty} P_{ESS}\,(t) = P_{ESS}^{ss} \quad (14)$$

where $P_{ESS}^{ss}$ is the steady-state control signal. Since the trajectory of $\dot{P}_{ESS}\,(t)$ resembles the impulse response, $\dot{P}_{ESS}\,(t)$ can be approximated with a set of Laguerre functions, formulated as

$$\dot{P}_{ESS}\,(t) \approx \sum_{i=1}^{m} c_i l_i\,(t) = L(t)^T\eta \quad (15)$$

where $\eta$ is the vector coefficients, composed of $\eta = \left[c_1\ c_2\ \ldots\ c_m\right]^T$ and $l_i\,(t), i = 1, 2, \ldots, m$ are the set of orthonormal basis functions, expressed in [30]. Note that $m$ defines the number of Laguerre networks. Accordingly, in a vector form, one can express $L\,(t) = \left[l_1\,(t)\ l_2\,(t)\ \ldots\ l_m\,(t)\right]^T$. According to [30] and [37], the Laguerre function dynamics is expressed as

$$\dot{L}\,(t) = A_\lambda L\,(t) \quad (16)$$

where $A_\lambda = \begin{bmatrix} -\lambda & 0 & \ldots & 0 \\ -2\lambda & -\lambda & \ldots & 0 \\ \vdots & \ddots & \ddots & \vdots \\ -2\lambda & \ldots & -2\lambda & -\lambda \end{bmatrix} \in \mathbb{R}^{m\times m}$ and $\lambda$ represents the time scaling factor for the Laguerre functions whose value is $\lambda > 0$. Thus, the exact solution of (16) can be obtained as

$$L\,(t) = e^{A_\lambda}L\,(0) \quad (17)$$

where $L\,(0) = \sqrt{2\lambda}\left[1\ 1\ \ldots\ 1\right]^T$.

#### 1) COST FUNCTION EVALUATION

The cost function is formulated as a function of predicted state variables and control, which are weighted by

$Q = Q^T \geq 0$ and $R = R^T > 0$, respectively. Typically, these matrices are diagonal matrices to simplify the representation. The expression of the cost function is stated as

$$J = \int_0^{T_p} \left[ x(t+\varphi)^T Q x(t+\varphi) + \dot{P}_{ESS}(\varphi)^T R \dot{P}_{ESS}(\varphi) \right] d\varphi \tag{18}$$

The first term of (18) is the predicted state variables, whose solution is obtained as

$$x(t+\varphi) = e^{A\varphi} x(t) + \phi(\varphi)^T \eta \tag{19}$$

where

$$\phi(\varphi)^T = \int_0^{\varphi} e^{A(\varphi-\gamma)} B L(\gamma)^T d\gamma \tag{20}$$

Note that convolution integral expressed in (20) can be solved recursively by partitioning predicted time $T_p$ into arbitrary time intervals $\varphi = 0, k, 2k, \ldots, T_p$, as done in [30]. In single input system, $R$ is a scalar. Thus, the second term of (18) can be reformulated into

$$\begin{aligned} \int_0^{T_p} \dot{P}_{ESS}(\varphi)^T R \dot{P}_{ESS}(\varphi)\, d\varphi &\approx \int_0^{\infty} \eta^T L(\varphi) R L(\varphi)^T \eta d\varphi \\ &= \eta^T R \eta \end{aligned} \tag{21}$$

Note that the orthonormality of Laguerre function allows $\int_0^{\infty} L(\varphi) L_k(\varphi)^T d\varphi = I$.

Substituting (19) and (21) into (18) gives

$$J = \eta^T \Omega \eta + 2\eta^T \psi x(t) + x(t)^T \int_0^{T_p} e^{A^T \varphi} Q e^{A\varphi} d\varphi\, x(t) \tag{22}$$

where

$$\begin{aligned} \Omega &= \int_0^{T_p} \phi(\varphi) Q \phi(\varphi)^T d\varphi + R \\ &\approx \sum_{i=0}^{q} \phi(ik) Q \phi(ik)^T k + R \end{aligned} \tag{23}$$

$$\psi = \int_0^{T_p} \phi(\varphi) Q e^{A\varphi} d\varphi \approx \sum_{i=0}^{q} \phi(ik) Q e^{Aik} k \tag{24}$$

Note that $\Omega$ and $\psi$ expressed in the integral form can be approximated numerically. By defining the predicted time window $T_p = qk$, time interval $\varphi$ can be stated as $\varphi = 0, k, 2k, \ldots, qk$, where $k$ is a constant step size. The step size $k$ can be selected as small as possible.

The optimal solution minimizing (22) can be obtained by taking the partial derivative of the cost function with respect to $\eta$ as

$$\frac{\partial J}{\partial \eta} = 0 \rightarrow \eta = -\Omega^{-1} \psi x(t) \tag{25}$$

Consequently, the optimal trajectory of derivative of control at $\varphi$ can be expressed as

$$\dot{P}_{ESS}(t) = -L(t)^T \Omega^{-1} \psi x(t) \tag{26}$$

#### 2) EMBEDDING OBSERVER FOR STATE VARIABLES ESTIMATION

Replacing $x(t+\varphi)$ with the estimated state, $\hat{x}(t+\varphi)$ in (18) leads to (27)

$$J = \int_0^{T_p} \left[ \hat{x}(t+\varphi)^T Q \hat{x}(t+\varphi) + \dot{P}_{ESS}(\varphi)^T R \dot{P}_{ESS}(\varphi) \right] d\varphi \tag{27}$$

which after some algebraic manipulation, is also equivalent to

$$J = \hat{\eta}^T \Omega \hat{\eta} + 2\hat{\eta}^T \psi \hat{x}(t) + \hat{x}(t)^T \int_0^{T_p} e^{A^T \varphi} Q e^{A\varphi} d\varphi\, \hat{x}(t) \tag{28}$$

where $\hat{\eta}$ denotes the estimated vector coefficient. Accordingly, the optimal $\hat{\eta}$ minimizing (28) is obtained as

$$\hat{\eta} = -\Omega^{-1} \psi \hat{x}(t) \tag{29}$$

Note that the difference between $\eta$ in (25) and $\hat{\eta}$ in (29) lie on the use of all state variables measurement. Once $\hat{x}(t)$ converges to $x(t)$, then $\hat{\eta}$ resembles to $\eta$.

#### 3) RECEDING HORIZON CONTROL

The basic concept of receding horizon control (RHC) is as follows: Once the set of the future control is obtained on a fixed predicted time window, $[0, qk]$, only the first one is adopted as the current control law. The principle of receding horizon control relies on the utilization of control signal at $\varphi = 0$. Thus, the derivative of control can be represented as

$$\dot{P}_{ESS}(t) = K_{mpc} \hat{x}(t) \tag{30}$$

where $K_{mpc} = -L(0)^T \Omega^{-1} \psi$ is known as a feedback gain matrix.

### B. MODEL PREDICTIVE FAST FREQUENCY CONTROL WITH CONSTRAINTS

In practical situations, the power of an energy storage system is restricted under specified limits. These limitations are considered as actuator constraints and they need to be incorporated to the control formulation to satisfy the control objective. Furthermore, to maintain the system frequency standard, the allowable range of the system frequency is included in the control design. Accordingly, the constraints are categorized into three terms, i.e. power limitation of energy storage, rate of power limitation of energy storage, and system frequency. These constraints are formulated into linear inequalities, which are necessary to provide boundary conditions for real-time optimization. The procedures of formulating the constraints into linear inequalities are described as follows:

#### 1) RATE OF POWER LIMITATION OF ENERGY STORAGE

The rate of power of ESS, $\dot{P}_{ESS}$, can be defined as the ESS ramp rate, whose unit is denoted in MW/s. The value of ESS ramp rate affects the characteristics of ESS to inject the power during disturbance. For instance, the high ramping capability of ESS is quicker to ramp up and reach maximum power during the initialization. On the other hand, slow ramping capability of ESS may induce to slower time required for the ESS to reach maximum power, which affects the frequency nadir and transient time. In general, the ramp rate of ESS is limited to

$$P_{RR,dn} \leq \dot{P}_{ESS}(t) \leq P_{RR,up} \tag{31}$$

where $P_{RR,up}$ and $P_{RR,dn}$ denote up and down ramp rates, respectively.

Employing the approximation of (26), at $t = 0$, (31) can be written as

$$-L(0)^T \hat{\eta} \leq -P_{RR,dn} \tag{32a}$$
$$L(0)^T \hat{\eta} \leq P_{RR,up} \tag{32b}$$

#### 2) POWER LIMITATION OF ENERGY STORAGE

It is known that an ESS is a limited capacity device, in which the power is restricted under its specification. Generally, it can be expressed as

$$P_{C,\max} \leq P_{ESS}(t) \leq P_{D,\max} \tag{33}$$

Accordingly, the ramp rate is expressed as

$$\dot{P}_{ESS}(t) = \frac{P_{ESS}(t) - P_{ESS}(t - T_s)}{T_s} = L(0)^T \hat{\eta} \tag{34}$$

where $T_s$ is the specified sampling time. Consequently, the ESS power at sampling instant $t$ can be represented as

$$P_{ESS}(t) = P_{ESS}(t - T_s) + L(0)^T \hat{\eta} T_s \tag{35}$$

Hence, substituting (35) into inequality (33) gives

$$P_{C,\max} - P_{ESS}(t - T_s) \leq L(0)^T \hat{\eta} T_s \leq P_{D,\max} - P_{ESS}(t - T_s) \tag{36}$$

(36) can be alternatively written as

$$-L(0)^T \hat{\eta} T_s \leq -P_{C,\max} + P_{ESS}(t - T_s) \tag{37a}$$
$$L(0)^T \hat{\eta} T_s \leq P_{D,\max} - P_{ESS}(t - T_s) \tag{37b}$$

#### 3) ALLOWABLE SYSTEM FREQUENCY

The allowable frequency deviation range is represented as

$$y_{\min} \leq C\hat{x}(t + \varphi) \leq y_{\max} \tag{38}$$

where $y_{\min}$ and $y_{\max}$ reflect minimum and maximum frequency deviations, respectively. Note that these values usually follow the grid code of certain regions or nations. For instance in Taiwan, the allowable frequency deviation is $\pm 0.5$ Hz. Substituting (19) into (38) yields

$$y_{\min} \leq C\left[e^{A\varphi}\hat{x}(t) + \phi(\varphi)^T \hat{\eta}\right] \leq y_{\max}, \tag{39}$$

which is equivalent to

$$y_{\min} - Ce^{A\varphi}\hat{x}(t) \leq C\phi(\varphi)^T \hat{\eta} \leq y_{\max} - Ce^{A\varphi}\hat{x}(t) \tag{40}$$

Consequently, (40) can be elaborated to

$$-C\phi(\varphi)^T \hat{\eta} \leq -y_{\min} + Ce^{A\varphi}\hat{x}(t) \tag{41a}$$
$$C\phi(\varphi)^T \hat{\eta} \leq y_{\max} - Ce^{A\varphi}\hat{x}(t) \tag{41b}$$

#### 4) COST FUNCTION EVALUATION

Recall that the cost function (22) with estimated state variables yielded by the observer contains the term

$$\hat{x}(t)^T \int_0^{T_p} e^{A^T\varphi} Q e^{A\varphi} d\varphi \hat{x}(t), \tag{42}$$

which can be considered as a constant, and consequently, the cost function of (28) can be written as (43).

$$\min_{\hat{\eta}} = \hat{\eta}^T \Omega \hat{\eta} + 2\hat{\eta}^T \psi \hat{x}(t) \tag{43}$$

subjected to

$$M\hat{\eta} \leq \beta \tag{44}$$

where $M$ and $\beta$ are the vectors whose elements are composed by the ESS power limitations and allowable system frequency, defined in (32), (37), and (41) as

$$M = \begin{bmatrix} -L(0)^T \\ L(0)^T \\ -L(0)^T T_s \\ L(0)^T T_s \\ -C\phi(\varphi)^T \\ C\phi(\varphi)^T \end{bmatrix}$$

$$\beta = \begin{bmatrix} -P_{RR,dn} \\ P_{RR,up} \\ -P_{C,\max} + P_{ESS}(t - T_s) \\ P_{D,\max} - P_{ESS}(t - T_s) \\ -y_{\min} + Ce^{A\varphi}\hat{x}(t) \\ y_{\max} - Ce^{A\varphi}\hat{x}(t) \end{bmatrix}$$

In other words, the numerical solution of this method is concerned with the problems of constrained minimization where the cost function is a positive definite quadratic function and constraint functions are linear functions. A QP approach can be applied to obtain such solutions.

## IV. PARAMETER IDENTIFICATION AND DETERMINATION FOR TAIPOWER SYSTEM

According to (1), the relationship between the frequency deviation to electrical power change can be described as

$$\frac{\tilde{f}(s)}{\tilde{P}_e(s)} = \frac{-\frac{1}{2H}s - \frac{1}{2HT_g}}{s^2 + \left(\frac{DT_g + 2H}{2HT_g}\right)s + \frac{1}{2HT_g}\left(D + \frac{1}{R_g}\right)} \tag{45}$$

From (45), one may observe that the lumped power system and governor can be represented into an approximate SISO system using generation and load aggregation. The unknown

parameters that need to be estimated are $H$, $D$, $T_g$, and $R_g$. By defining the system model with second order system as

$$\frac{\tilde{f}_m(s)}{\tilde{P}_e(s)} = \frac{-a_1 s - a_0}{s^2 + b_1 s + b_0} \tag{46}$$

where $\tilde{f}_m$ is the frequency deviation obtained from system modeling. $a_0$ and $a_1$ denote the coefficient associated with the numerator whereas $b_0$ and $b_1$ represent the coefficient associated with the denominator. Accordingly, the corresponding unknown parameters can be estimated as

$$\begin{aligned} H &= \frac{1}{2a_1} \\ T_g &= \frac{a_1}{a_0} \\ D &= \frac{b_1 a_1 - a_0}{a_1^2} \\ R_g &= \frac{1}{\frac{b_0}{a_0} - \left(\frac{b_1 a_1 - a_0}{a_1^2}\right)} \end{aligned} \tag{47}$$

The estimated system parameters $a_0$, $a_1$, $b_0$, and $b_1$ are obtained via least squares method, which is describe as follows.

(46) can be re-written as

$$s^2\tilde{f}_m(s) + b_1 s\tilde{f}_m(s) + b_0\tilde{f}_m(s) = a_1 s(-\tilde{P}_e(s)) + a_0(-\tilde{P}_e(s)) \tag{48}$$

Taking the inverse of Laplace transform of (48) yields

$$\ddot{\tilde{f}}_m(t) + b_1\dot{\tilde{f}}_m(t) + b_0\tilde{f}_m(t) = a_1(-\dot{\tilde{P}}_e(t)) + a_0(-\tilde{P}_e(t)), \tag{49}$$

which is also equivalent to

$$\tilde{f}_m(t) = -\frac{1}{b_0}\ddot{\tilde{f}}_m(t) - \frac{b_1}{b_0}\dot{\tilde{f}}_m(t) + \frac{a_1}{b_0}(-\dot{\tilde{P}}_e(t)) + \frac{a_0}{b_0}(-\tilde{P}_e(t)) \tag{50}$$

Thus, (50) can also be represented in a matrix form as

$$\tilde{f}_m(t) = \Phi(t)\,\mu \tag{51}$$

where $\Phi$ denotes the regressor and $\mu$ represents a vector containing the unknown parameters. Their elements can be rewritten as

$$\begin{aligned} \Phi(t) &= \left[\ddot{\tilde{f}}_m(t)\ \dot{\tilde{f}}_m(t)\ -\dot{\tilde{P}}_e(t)\ -\tilde{P}_e(t)\right] \\ \mu &= \left[-\tfrac{1}{b_0}\ -\tfrac{b_1}{b_0}\ \tfrac{a_1}{b_0}\ \tfrac{a_0}{b_0}\right]^T \end{aligned}$$

Since the element of the regressor is essentially known and is based on the measurement data, the element of the regressor containing $\ddot{\tilde{f}}_m(t)$ and $\dot{\tilde{f}}_m(t)$ can be replaced by $\ddot{\tilde{f}}(t)$ and $\dot{\tilde{f}}(t)$, respectively. Consequently, it results in

$$\Phi(t) = \left[\ddot{\tilde{f}}(t)\ \dot{\tilde{f}}(t)\ -\dot{\tilde{P}}_e(t)\ -\tilde{P}_e(t)\right]$$

Defining the modeling error as the difference between the actual data and model, stated as

$$\upsilon = \tilde{f}(t) - \tilde{f}_m(t) \tag{52}$$

A cost function, which defines the function of modeling error, is formulated as

$$\begin{aligned} J_{LS} &= \upsilon^T\upsilon \\ &= \left[\tilde{f}(t) - \Phi(t)\,\mu\right]^T\left[\tilde{f}(t) - \Phi(t)\,\mu\right] \\ &= \left[\tilde{f}(t)^T - \mu^T\Phi(t)^T\right]\left[\tilde{f}(t) - \Phi(t)\,\mu\right] \\ &= \tilde{f}(t)^T\tilde{f}(t) - 2\mu^T\Phi(t)^T\tilde{f}(t) + \mu^T\Phi(t)^T\Phi(t)\,\mu \end{aligned} \tag{53}$$

$J_{LS}$, minimizing $\mu$, can be obtained by taking the partial derivative of $J_{LS}$ with respect to $\mu$ as

$$\frac{\partial J_{LS}}{\partial \mu} = -2\Phi(t)^T\left[\tilde{f}(t) - \Phi(t)\,\mu\right] = 0 \tag{54}$$

Accordingly, the optimal $\mu$ can be obtained as

$$\mu_{opt} = \left(\Phi(t)^T\Phi(t)\right)^{-1}\Phi(t)^T\tilde{f}(t) \tag{55}$$

The validation of the proposed method is conducted for Taiwan power systems. Two events recorded in PMUs occurred on September 14, 2018 (event 1) and December 1, 2018 (event 2) are taken as examples of generation-loss cases. Event 1 dealt with three generator units trip whose total power generation is 708 MW. On the other hand, one generator unit is tripped with total power generation of 550 MW in event 2.

Figure 2 shows the frequency responses recorded from the PMU, resulted from two actual generation-loss events. The sampled time of PMU is 0.05 s. The figure shows that the models obtained from system identification technique are in great agreement with the real measurement data.

The total system loads of events 1 and 2 are 32607 and 24127 MW, respectively. The model for even 2 is stated in (56).

$$\frac{\tilde{f}(s)}{\tilde{P}_e(s)} = \frac{-0.0446s - 0.0075}{s^2 + 0.1889s + 0.0381} \tag{56}$$

The corresponding estimated power system parameters are obtained as $H = 11.22$, $D = 0.48$, $R_g = 0.22$, and $T_g = 5.97$ based on calculation in [33].

Table 1 lists parameters of the proposed method. The weighting matrices $Q = Q^T \in \mathbb{R}^{3\times3}$ and $R \in \mathbb{R}^{1\times1}$ are associated with the predicted state variables and the time derivative of the control input, respectively. The optimal Q is often selected as $Q = C^TC$ [28]. With this choice, the closed-loop eigenvalues are determined by $R$. The larger $R$ generates the smaller control input, which results in slower settling time. On the contrary, the smaller $R$ produces the higher control input, which yields fast response, yet exhibits overshoot.

Fig. 3 shows the frequency trajectory of the power system under various time-delay constants. As can be seen, the maximum time-delay causing the system to be marginally

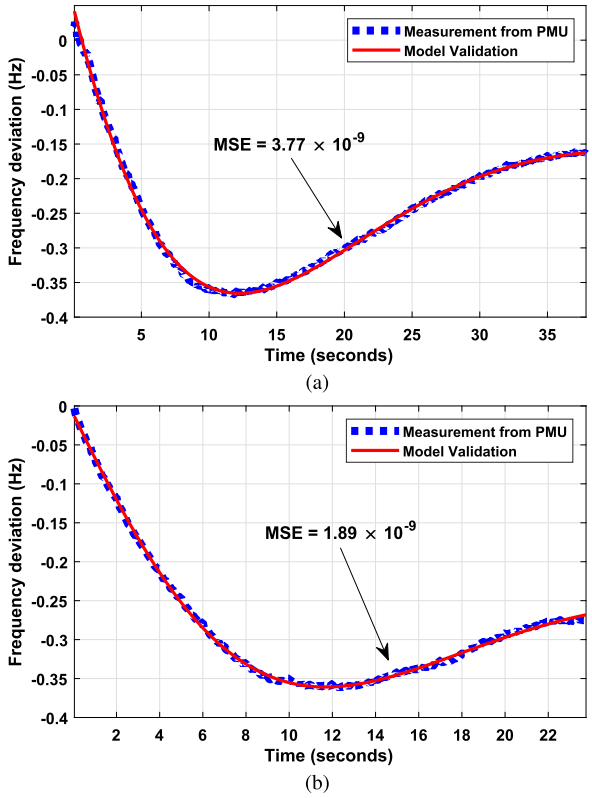


**FIGURE 2.** Actual contingencies occurred in Taiwan: (a) Event 1, (b) Event 2.

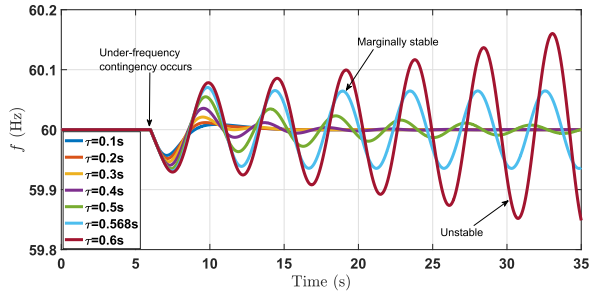


**FIGURE 3.** Frequency trajectory under various time-delay constants.

stable is $\tau = 0.568$s. This indicates that MP-FFC is unable to compensate the time-delay, which is greater than $\tau = 0.568$s.

Changes of system parameters are also a key factor contributing to the shift of the critical time-delay. To validate this, the MP-FFC designed for event 2 is tested to event 1, whose system parameters are different from event 2. In event 1, the system parameters are obtained as follows: $H = 8.92$, $D = 2.09$, $R_g = 0.19$, and $T_g = 24.14$. Accordingly, as depicted in Fig. 4, the critical time-delay shifts to 0.49s, which is smaller than the previous one. This indicates that system uncertainties can affect the critical time-delay.

## V. CASE STUDIES

To verify the robustness of the proposed method in compensating the TDSAs, four cases studies are carried out and

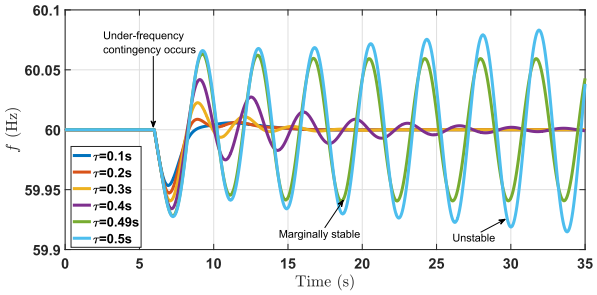


**FIGURE 4.** Frequency trajectory under various time-delay constants for case where the system parameters change.

two types of TDSA, i.e. constant and random TDSAs are investigated. The first and second cases are to study the robustness of the proposed controller against constant and random TDSAs, respectively. On the other hand, the robustness of the proposed controller under parameter variations, together with constant and random TSDAs, is investigated in cases 3 and 4, respectively. It is to be noted that these TDSAs occur at $t = 0$s, which are subsequently followed by an under-frequency contingency (i.e. generator outage) at $t = 6$s. Moreover, to justify the proposed method, three controllers are tested under these cases. The first controller is named as model predictive FFC (MP-FFC) without constraints. It is based on the model developed in most of the studies such as [38], [39] where the time-delay estimator and corrector are not included in the control formulation. Moreover, the system constraints such as the ESS limitation and frequency constraints are also not taken into account. The second control is called improved model predictive FFC (IMP-FFC) without constraints. Different from MPC-FFC, IMP-FFC employs the proposed time-delay estimator (i.e. ST-TDE) and corrector (i.e. SSP). Finally, the third controller is the complete proposed controller, which is called IMP-FFC with constraints. It consists of the model predictive control together with the proposed SSP and ST-TDE, and takes the system constraints into account as well.

### A. ROBUSTNESS AGAINST CONSTANT TIME-DELAY SWITCH ATTACK

The constant TDSA is set to $\tau(t) = 5$s. The TDSA value is selected greater than the critical time-delay (about 8.8 times) to prove the robustness of the proposed method. Fig. 5a depicts the trajectory of frequency under constant TDSA and generator outage. As can be seen, the MP-FFC without constraints causes the frequency to diverge from its nominal value and results in unstable response since the value of TDSA is larger than the critical time-delay that can be withstood by the corresponding controller. It is indicated that at $t = 6$s, the frequency response of MP-FFC causes the frequency uncontrollably oscillates. On the other hand, the proposed method is able to regulate the frequency in the presence of TDSA and under-frequency contingency by accurately estimating the unknown TDSA and effectively

**TABLE 1. Parameters of the proposed method.**

| Subsystem | Parameters |
|---|---|
| Model Predictive Control | $Q = C^T C$; $R = 0.01$; $\lambda = 0.2$; $m = 6$; $T_p = 10$; $K_{ob} = \begin{bmatrix} 439.81 & 24.3 & 8.81 \end{bmatrix}^T$ |
| Sequential State Predictor | $N = 40$ $K_{SP1} = \ldots = K_{SPN} = \begin{bmatrix} -4 & 0 & 0 \\ 0 & -4 & 0 \\ 0 & 0 & -4 \end{bmatrix}$ |
| Super-Twisting Time-Delay Estimator | $\alpha_1 = 100$ $\alpha_2 = 20$ |

**TABLE 2. Power limitation of ESS and frequency deviation constraints.**

| Parameters | Symbol | Value | Unit |
|---|---|---|---|
| Max. charging power | $P_{C,\max}$ | $-554.92$ | MW |
| Max. discharging power | $P_{D,\max}$ | 554.92 | MW |
| Down ramp rate | $P_{RR,dn}$ | $-72.38$ | MW/s |
| Up ramp rate | $P_{RR,up}$ | 72.38 | MW/s |
| Min. frequency deviation | $y_{\min}$ | $-0.5$ | Hz |
| Max. frequency deviation | $y_{\max}$ | 0.5 | Hz |

compensating the actual TDSA based on the estimated TDSA. As depicted in Fig. 5b, the estimated TDSA can converge to the actual TDSA within 5s from its initial value. Note that the initial value is selected as the minimum time-delay which can possibly occur in the system. Moreover, compared to the proposed method, IMP-FFC without constraints yields high overshoot frequency response, yet producing the same frequency nadir, that is 59.64 Hz.

In terms of constraint handling, the $P_{ESS}$ generated by the proposed method satisfies the range of the specified power limitation. Figs. 5c and 6 justify the effectiveness of the proposed method in distributing the ESS power and its ramp rates. As can be seen, the proposed method is capable of optimally allocating $P_{ESS}$ under given power limitations. On the contrary, the other two methods are not able to allocate $P_{ESS}$ under its limitation, as $P_{ESS}$ specifications are not incorporated in the controller design. This emphasizes the importance of incorporating $P_{ESS}$ specifications into control design to attain the feasible optimal values.

### B. ROBUSTNESS AGAINST RANDOM TIME-DELAY SWITCH ATTACK

The random TDSA is given within the range $\tau\ (t) = [3, 5.5]$s with sample time 0.1s. This range is selected since it is greater than the critical time-delay, which essentially causes the power system to be unstable.

Fig. 7a shows the trajectory of system frequency under random TDSA and generator outage. As can be seen, the proposed method is able to maintain and stabilize the system frequency under random TDSA. Furthermore, the system frequency can also be recovered to its nominal value by the proposed method, while the other two controllers are not able to stabilize the system under random TDSA. Additionally, the unknown and random TDSA can also be accurately estimated

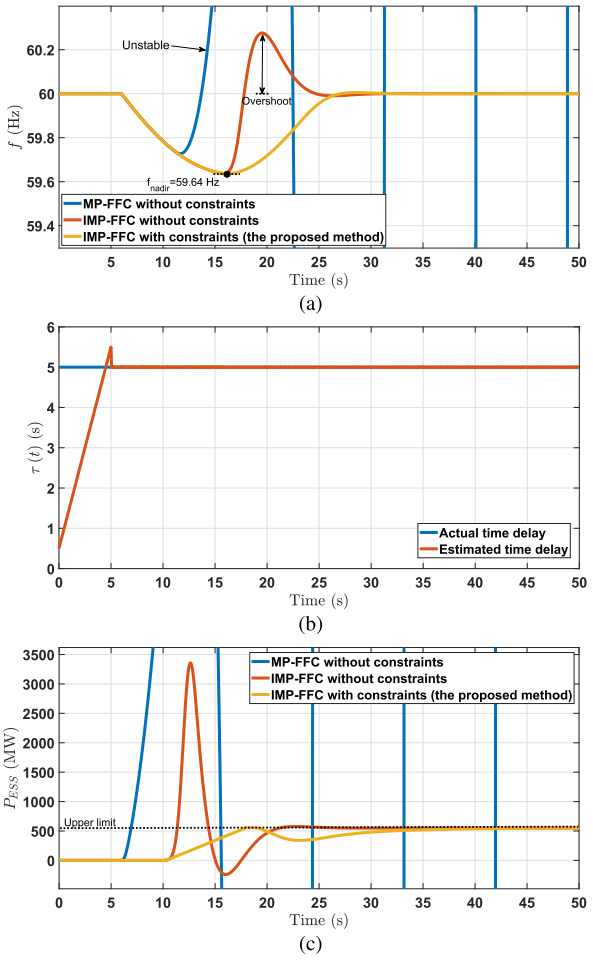


**FIGURE 5. Trajectories of: (a) $f$; (b) $P_{ESS}$; and (c) $\hat{\tau}$ under constant time-delay switch attack.**

by the proposed method. As depicted in Fig. 8, the resulting time-delay estimation produced by the proposed method can quickly converge to the actual TDSA.

The proposed method is also able to allocate $P_{ESS}$, satisfying the range of the specified power limitation. As evident in Figs. 7(b) and 9, the ESS power and ramp rate generated by the proposed method are still within the specified limits. This indicates that the proposed method is able to handle the constraints determined by the ESS specifications.

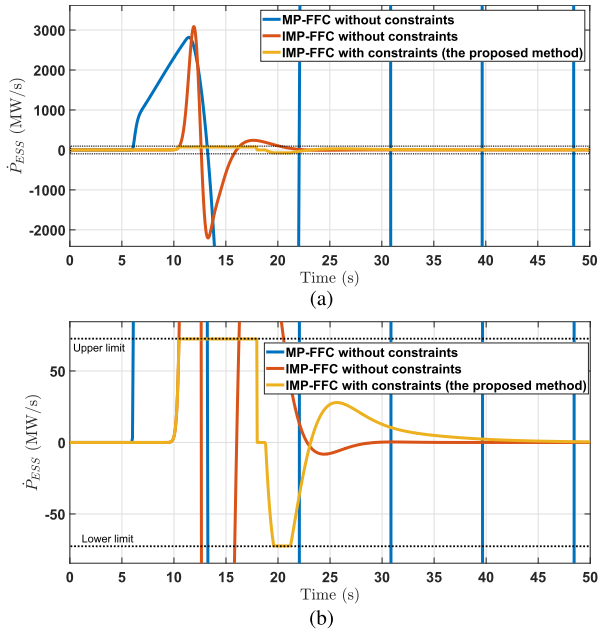


**FIGURE 6.** Trajectories of: (a) $\dot{P}_{ESS}$; (b) $\dot{P}_{ESS}$ (zoom-in) under constant time-delay switch attack.

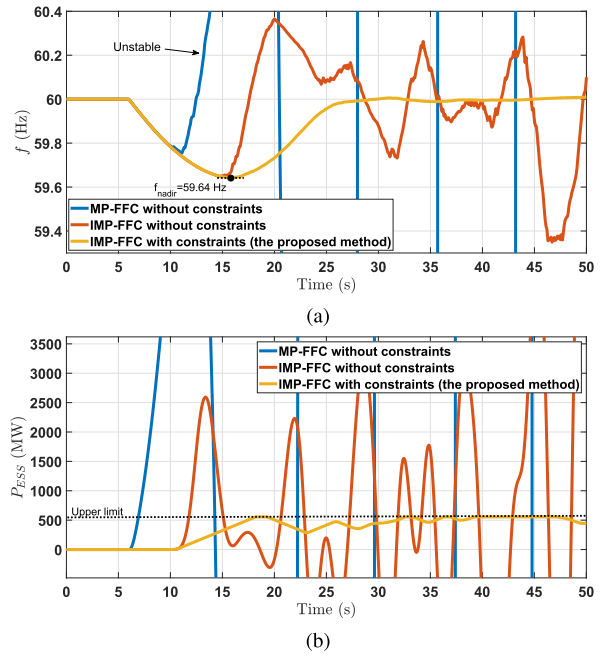


**FIGURE 7.** Trajectories of: (a) $f$; and (b) $P_{ESS}$ under random time-delay switch attack.

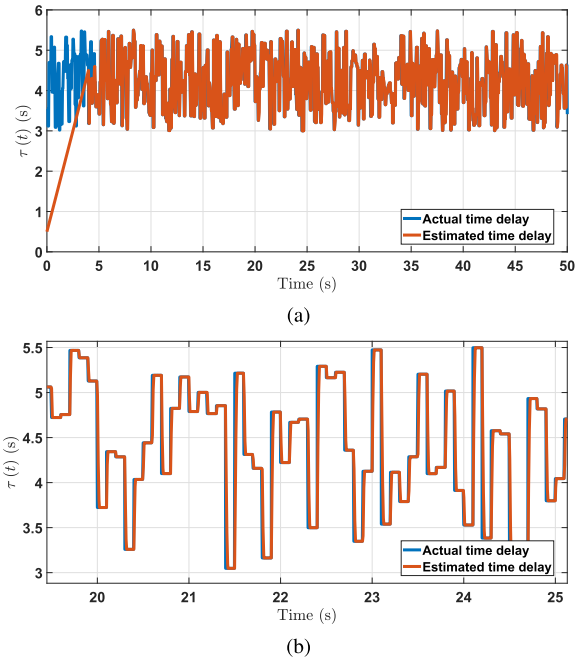


**FIGURE 8.** Trajectories of: (a) $\hat{\tau}$; and (b) $\hat{\tau}$ (zoom-in) under random time-delay switch attack.

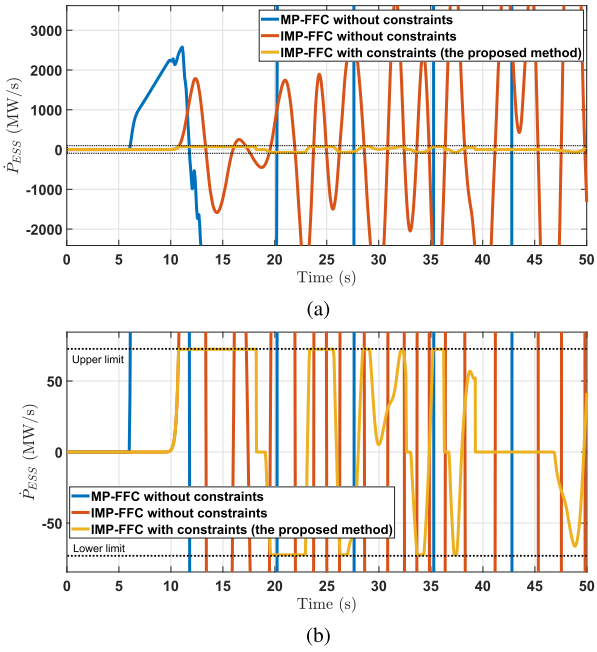


**FIGURE 9.** Trajectories of: (a) $\dot{P}_{ESS}$; (b) $\dot{P}_{ESS}$ (zoom-in) under random time-delay switch attack.

### C. CASE 3: ROBUSTNESS UNDER PARAMETER VARIATIONS AND CONSTANT TIME-DELAY SWITCH ATTACK

In this case, the controller parameters determined by the parametric identification of event 2 are subsequently applied for event 1. Note that events 1 and 2 occurred at different days of the year. Hence, the system inertia, total demanded power, and etc. are completely different. This case study is aimed at testing the robustness of the proposed method to counteract the system parameter and external disturbance variations as well as the constant TDSA. The constant TDSA is set to $\tau\,(t) = 5$s from $t = 0$. The power limitations of ESS for this case are listed in Table 3. Figure 10(a) depicts the trajectories of the system frequency. As can be seen, the IMP-FFC with constraints is able to stabilize the power systems. The frequency nadir governed by the IMP-FFC with

**TABLE 3. Power limitation of ESS for Cases 3 and 4.**

| Parameters | Symbol | Value | Unit |
|---|---|---|---|
| Max. charging power | $P_{C,\max}$ | 749.85 | MW |
| Max. discharging power | $P_{D,\max}$ | 749.85 | MW |
| Max. charging ramp rate | $\dot{P}_{C,\max}$ | 97.8 | MW/s |
| Max. discharging ramp rate | $\dot{P}_{D,\max}$ | 97.8 | MW/s |

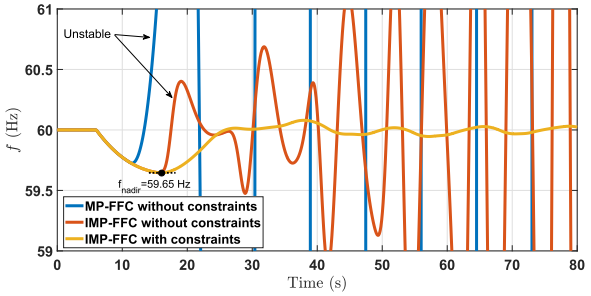


(a)

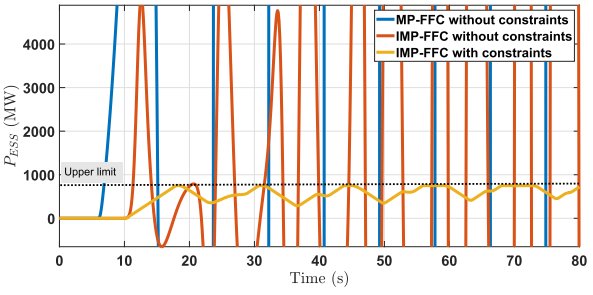


(b)

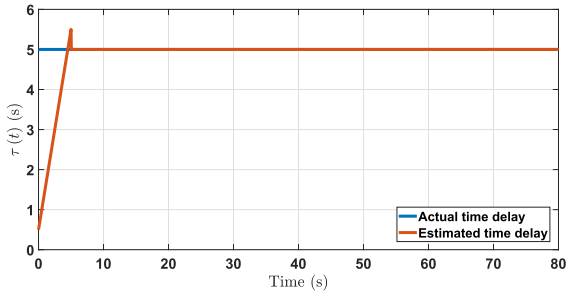


(c)

**FIGURE 10. Trajectories of: (a) $f$; (b) $P_{ESS}$; and (c) $\hat{\tau}$ under parameter variations and constant time-delay switch attack.**

constraints can be rescued to 59.65 Hz. Moreover, as illustrated in Figures 10(b) and 11, $P_{ESS}$ and $\dot{P}_{ESS}$ generated by the IMP-FFC with constraints satisfies the ESS power limitations. It can be indicated that the resulting $P_{ESS}$ and $\dot{P}_{ESS}$ are still within the limits. On the contrary, both MP-FFC and IMP-FFC without constraints are not able to produce $P_{ESS}$ and $\dot{P}_{ESS}$ satisfying the specified limits. Accordingly, both controllers are not able to maintain the system stability. As demonstrated in Figure 10(c), the estimated time-delay can converge to actual time-delay, whose initial settling time is similar to that of Case 1. Hence, it justifies that system parameter variations do not affect the STA TDE.

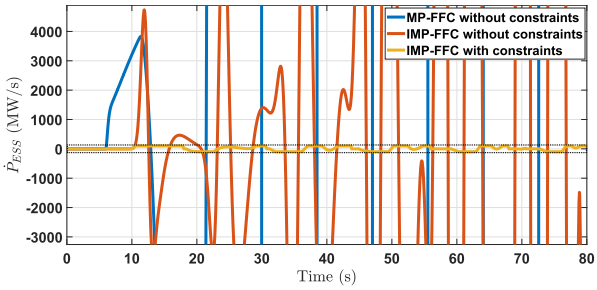


(a)

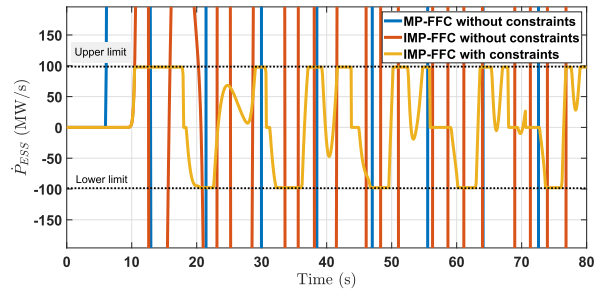


(b)

**FIGURE 11. Trajectories of: (a) $\dot{P}_{ESS}$; (b) $\dot{P}_{ESS}$ (zoom-in) under parameter variations and constant time-delay switch attack.**

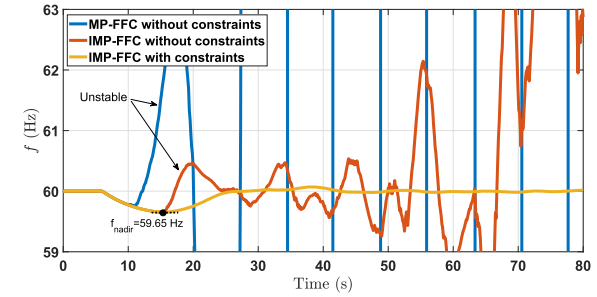


(a)

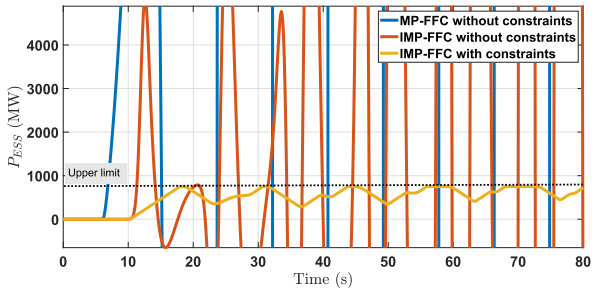


(b)

**FIGURE 12. Trajectories of: (a) $f$; and (b) $P_{ESS}$ under parameter variations and random time-delay switch attack.**

### D. CASE 4: ROBUSTNESS UNDER PARAMETER VARIATIONS AND RANDOM TIME-DELAY SWITCH ATTACK

In this case, the system is tested under parameter variations, whose setup is the same as that of Case 3. However, random TDSA is injected at $t = 0$, whose value range is the same as that of Case 2. The power limitations of ESS for this case are listed in Table 3.

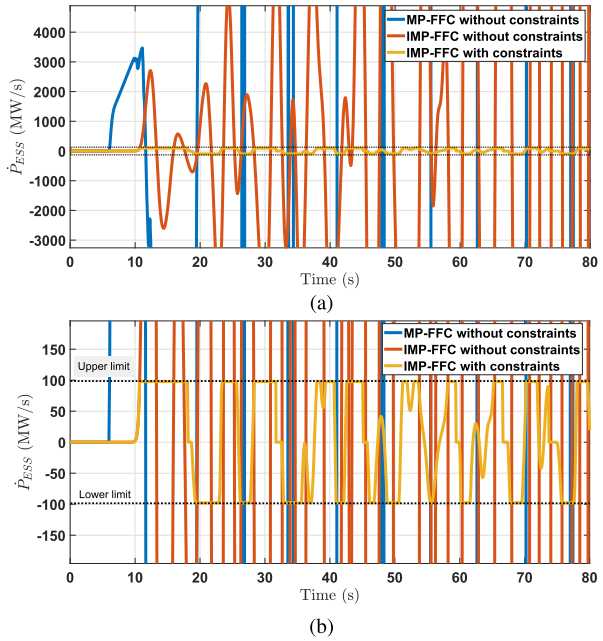


**FIGURE 13.** Trajectories of: (a) $\dot{P}_{ESS}$; (b) $\dot{P}_{ESS}$ (zoom-in) under parameter variations and random time-delay switch attack.

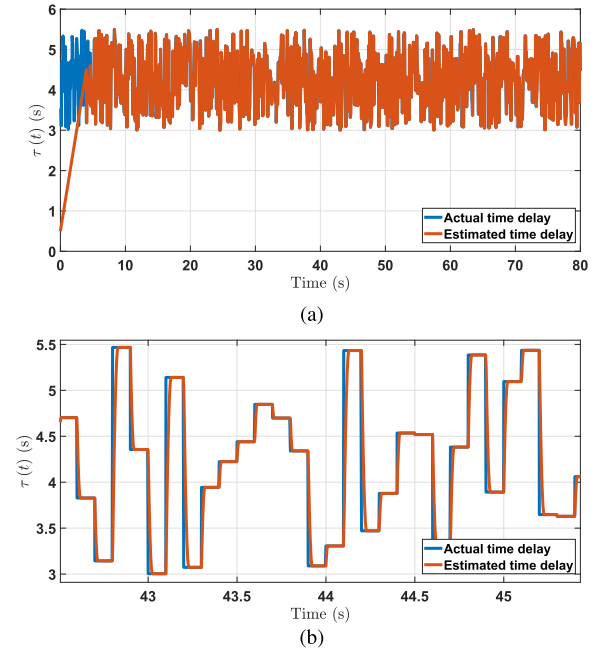


**FIGURE 14.** Trajectories of: (a) $\hat{\tau}$; and (b) $\hat{\tau}$ (zoom-in) under parameter variations and random time-delay switch attack.

The system frequency trajectory is shown in Figure 12(a). As can be seen, the IMP-FFC with constraints maintains the frequency and is able to regulate the frequency to its nominal value after 18s. Moreover, the frequency nadir can be rescued to 59.65Hz, which is still within the Taipower standard. This proves the superiority of the IMP-FFC with constraints in counteracting random TDSA and handling the ESS power limitations. On the contrary, both MP-FFC and IMP-FFC without constraints are not able to stabilize the frequency. The frequency trajectories yielded by these methods tend to diverge and exhibit severe oscillations.

In terms of constraints handling, the IMP-FFC with constraints is able to satisfy the constraints given by ESS specifications. As can be seen from Figures 12(b) and 13, the IMP-FFC with constraints is able to allocate $P_{ESS}$ and $\dot{P}_{ESS}$ within their specified ranges. On the other hand, both MP-FFC and IMP-FFC without constraints are not able to allocate $P_{ESS}$ and $\dot{P}_{ESS}$ within their specified ranges since the constraints are not considered in their control design.

Furthermore, the random TDSA can be accurately estimated via STA TDE as shown in Figure 14. By accurately estimating the unknown TDSA, the controllers can provide control actions corresponding to the estimated TDSA.

## VI. CONCLUSION

In this paper, a unified fast frequency control, based on model predictive control has been proposed. The proposed method is not only able to regulate the system frequency to the nominal value during large disturbance, but also able to counteract any types of unknown TDSA. By accurately estimating the unknown TDSA, the proposed method can compensate the attacks injected by the hacker. Thus, the power system resiliency can be maintained. Furthermore, the proposed method is also able to optimally allocate ESS power based on ESS specifications, such as ESS power and ramp rate, and frequency limits set by the grid code.

## REFERENCES

[1] M. Victorio, A. Sargolzaei, and M. R. Khalghani, "A secure control design for networked control systems with linear dynamics under a time-delay switch attack," *Electronics*, vol. 10, no. 3, p. 322, Jan. 2021. [Online]. Available: https://www.mdpi.com/2079-9292/10/3/322

[2] A. Sargolzaei, K. K. Yen, and M. N. Abdelghani, "Preventing time-delay switch attack on load frequency control in distributed power systems," *IEEE Trans. Smart Grid*, vol. 7, no. 2, pp. 1176–1185, Mar. 2016.

[3] X.-C. Shangguan, Y. He, C.-K. Zhang, W. Yao, Y. Zhao, L. Jiang, and M. Wu, "Resilient load frequency control of power systems to compensate random time delays and time-delay attacks," *IEEE Trans. Ind. Electron.*, early access, Jul. 1, 2022, doi: 10.1109/TIE.2022.3186335.

[4] L. Jiang, W. Yao, Q. H. Wu, J. Y. Wen, and S. J. Cheng, "Delay-dependent stability for load frequency control with constant and time-varying delays," *IEEE Trans. Power Syst.*, vol. 27, no. 2, pp. 932–941, May 2012.

[5] C.-K. Zhang, L. Jiang, Q. H. Wu, Y. He, and M. Wu, "Further results on delay-dependent stability of multi-area load frequency control," *IEEE Trans. Power Syst.*, vol. 28, no. 4, pp. 4465–4474, Nov. 2013.

[6] F. Yang, J. He, and Q. Pan, "Further improvement on delay-dependent load frequency control of power systems via truncated B–L inequality," *IEEE Trans. Power Syst.*, vol. 33, no. 5, pp. 5062–5071, Sep. 2018.

[7] S. Sönmez and S. Ayasun, "Stability region in the parameter space of PI controller for a single-area load frequency control system with time delay," *IEEE Trans. Power Syst.*, vol. 31, no. 1, pp. 829–830, Jan. 2016.

[8] S. Sönmez, S. Ayasun, and C. O. Nwankpa, "An exact method for computing delay margin for stability of load frequency control systems with constant communication delays," *IEEE Trans. Power Syst.*, vol. 31, no. 1, pp. 370–377, Jan. 2016.

[9] C. Fu, C. Wang, L. Y. Wang, and D. Shi, "An alternative method for mitigating impacts of communication delay on load frequency control," *Int. J. Electr. Power Energy Syst.*, vol. 119, Jul. 2020, Art. no. 105924. [Online]. Available: https://www.sciencedirect.com/science/article/pii/S0142061519339729

[10] K. S. Xiahou, Y. Liu, and Q. H. Wu, "Robust load frequency control of power systems against random time-delay attacks," *IEEE Trans. Smart Grid*, vol. 12, no. 1, pp. 909–911, Jan. 2021.
[11] X. M. Ren, A. B. Rad, P. T. Chan, and W. L. Lo, "Online identification of continuous-time systems with unknown time delay," *IEEE Trans. Autom. Control*, vol. 50, no. 9, pp. 1418–1422, Sep. 2005.
[12] S. Diop, I. Kolmanovsky, P. E. Moraal, and M. Van Nieuwstadt, "Preserving stability/performance when facing an unknown time-delay," *Control Eng. Pract.*, vol. 9, no. 12, pp. 1319–1325, Dec. 2001. [Online]. Available: https://www.sciencedirect.com/science/article/pii/S0967066101000788
[13] D. Etter and S. Stearns, "Adaptive estimation of time delays in sampled data systems," *IEEE Trans. Acoust., Speech, Signal Process.*, vol. ASSP-29, no. 3, pp. 582–587, Jun. 1981.
[14] J. Herrera and A. Ibeas, "On-line delay estimation for stable, unstable and integrating systems under step response," *ISA Trans.*, vol. 51, no. 3, pp. 351–361, 2012. [Online]. Available: https://www.sciencedirect.com/science/article/pii/S0019057811001327
[15] Y. Deng, V. Lechappe, E. Moulay, and F. Plestan, "Prediction-based control with delay estimation of LTI systems with input-output delays," in *Proc. Amer. Control Conf. (ACC)*, Jul. 2019, pp. 3702–3707.
[16] V. Léchappé, S. Rouquet, A. González, F. Plestan, J. De León, E. Moulay, and A. Glumineau, "Delay estimation and predictive control of uncertain systems with input delay: Application to a DC motor," *IEEE Trans. Ind. Electron.*, vol. 63, no. 9, pp. 5849–5857, Sep. 2016.
[17] L. Belkoura, "Identifiabilty of systems described by convolution equations," *Automatica*, vol. 41, no. 3, pp. 505–512, 2005. [Online]. Available: https://www.sciencedirect.com/science/article/pii/S0005109804003309
[18] L. Belkoura and J.-P. Richard, "A distribution framework for the fast identification of linear systems with delays," *IFAC Proc. Volumes*, vol. 39, no. 10, pp. 132–137, 2006. [Online]. Available: https://www.sciencedirect.com/science/article/pii/S1474667016352053
[19] L. Belkoura, J.-P. Richard, and M. Fliess, "Parameters estimation of systems with delayed and structured entries," *Automatica*, vol. 45, no. 5, pp. 1117–1125, 2009. [Online]. Available: https://www.sciencedirect.com/science/article/pii/S0005109809000302
[20] D. Bresch-Pietri, J. Chauvin, and N. Petit, "Adaptive control scheme for uncertain time-delay systems," *Automatica*, vol. 48, no. 8, pp. 1536–1552, Aug. 2012. [Online]. Available: https://www.sciencedirect.com/science/article/pii/S0005109812002294
[21] D. Bresch-Pietri and M. Krstic, "Delay-adaptive predictor feedback for systems with unknown long actuator delay," *IEEE Trans. Autom. Control*, vol. 55, no. 9, pp. 2106–2112, Sep. 2010.
[22] Y. Zhu, H. Su, and M. Krstic, "Adaptive backstepping control of uncertain linear systems under unknown actuator delay," *Automatica*, vol. 54, pp. 256–265, Apr. 2015. [Online]. Available: https://www.sciencedirect.com/science/article/pii/S0005109815000667
[23] A. Abbasspour, A. Sargolzaei, M. Victorio, and N. Khoshavi, "A neural network-based approach for detection of time delay switch attack on networked control systems," *Proc. Comput. Sci.*, vol. 168, pp. 279–288, Jan. 2020. [Online]. Available: https://www.sciencedirect.com/science/article/pii/S1877050920303896
[24] Y. Tan, "Time-varying time-delay estimation for nonlinear systems using neural networks," *Int. J. Appl. Math. Comput. Sci.*, vol. 14, no. 1, pp. 63–68, 2004. [Online]. Available: http://eudml.org/doc/207680
[25] S. Drakunov, W. Perruquetti, J.-P. Richard, and L. Belkoura, "Delay identification in time-delay systems using variable structure observers," *Annu. Rev. Control*, vol. 30, no. 2, pp. 143–158, 2006. [Online]. Available: https://www.sciencedirect.com/science/article/pii/S1367578806000435
[26] Y. Deng, V. Léchappé, S. Rouquet, E. Moulay, and F. Plestan, "Super-twisting algorithm-based time-varying delay estimation with external signal," *IEEE Trans. Ind. Electron.*, vol. 67, no. 12, pp. 10663–10671, Dec. 2020.
[27] Y. Deng, V. Léchappé, E. Moulay, and F. Plestan, "Predictor-based control of LTI remote systems with estimated time-varying delays," *IEEE Control Syst. Lett.*, vol. 5, no. 1, pp. 289–294, Jan. 2021.
[28] A. Levant, "Sliding order and sliding accuracy in sliding mode control," *Int. J. Control*, vol. 58, no. 6, pp. 1247–1263, Dec. 1993, doi: 10.1080/00207179308923053.
[29] X.-C. Shangguan, C.-K. Zhang, Y. He, L. Jin, L. Jiang, J. W. Spencer, and M. Wu, "Robust load frequency control for power system considering transmission delay and sampling period," *IEEE Trans. Ind. Informat.*, vol. 17, no. 8, pp. 5292–5303, Aug. 2021.
[30] L. Wang, *Model Predictive Control System Design and Implementation Using MATLAB*. London, U.K.: Springer-Verlag, 2009.
[31] J. M. Maciejowski, *Predictive Control With Constraints*. Upper Saddle River, NJ, USA: Prentice-Hall, 2002.
[32] N. Sockeel, J. Gafford, B. Papari, and M. Mazzola, "Virtual inertia emulator-based model predictive control for grid frequency regulation considering high penetration of inverter-based energy storage system," *IEEE Trans. Sustain. Energy*, vol. 11, no. 4, pp. 2932–2939, Oct. 2020.
[33] R. K. Subroto, K.-L. Lian, C.-C. Chu, and C.-J. Liao, "A fast frequency control based on model predictive control taking into account of optimal allocation of power from the energy storage system," *IEEE Trans. Power Del.*, vol. 36, no. 4, pp. 2467–2478, May 2021.
[34] Z. Chen, Z. Liu, and L. Wang, "A modified model predictive control method for frequency regulation of microgrids under status feedback attacks and time-delay attacks," *Int. J. Electr. Power Energy Syst.*, vol. 137, May 2022, Art. no. 107713. [Online]. Available: https://www.sciencedirect.com/science/article/pii/S014206152100939X
[35] S. Pulendran and J. E. Tate, "Energy storage system control for prevention of transient under-frequency load shedding," *IEEE Trans. Smart Grid*, vol. 8, no. 2, pp. 927–936, Mar. 2017.
[36] G. Besancon, D. Georges, and Z. Benayache, "Asymptotic state prediction for continuous-time systems with delayed input and application to control," in *Proc. Eur. Control Conf. (ECC)*, 2007, pp. 1786–1791.
[37] L. Wang, "Continuous time model predictive control design using orthonormal functions," *Int. J. Control*, vol. 74, no. 16, pp. 1588–1600, Jan. 2001, doi: 10.1080/00207170110082218.
[38] D. Yang, "Inertia-adaptive model predictive control-based load frequency control for interconnected power systems with wind power," *IET Gener., Transmiss. Distrib.*, vol. 14, pp. 5029–5036, Nov. 2020. [Online]. Available: https://digital-library.theiet.org/content/journals/10.1049/iet-gtd.2020.0018
[39] U. Tamrakar, T. M. Hansen, R. Tonkoski, and D. A. Copp, "Model predictive frequency control of low inertia microgrids," in *Proc. IEEE 28th Int. Symp. Ind. Electron. (ISIE)*, Jun. 2019, pp. 2111–2116.

**RAMADHANI KURNIAWAN SUBROTO** (Member, IEEE) received the B.Eng. degree in electrical engineering from the Institut Teknologi Sepuluh Nopember, Surabaya, Indonesia, in 2012, the dual M.Eng. and M.Sc. degrees in electrical engineering from the Institut Teknologi Sepuluh Nopember and the National Taiwan University of Science and Technology, Taiwan, in 2014, and the Ph.D. degree from the National Taiwan University of Science and Technology, in 2021. He is currently a Postdoctoral Researcher with the Technical University of Denmark.

**KUO LUNG LIAN** (Senior Member, IEEE) received the B.A.Sc. (Hons.), M.A.Sc., and Ph.D. degrees in electrical engineering from the University of Toronto, in 2001, 2003, and 2007, respectively. He was a Visiting Research Scientist with the Central Research Institute of Electric Power Industry (CRIEPI), Japan, from October 2007 to January 2009. He is currently a Professor with the National Taiwan University of Science and Technology. He served as the Chairperson of the IAS at Taipei Chapter from 2019 to 2021. He is an Associate Editor of IEEE ACCESS and IEEE TRANSACTIONS ON POWER DELIVERY and an Assistant Editor of JCIE.